15-band spectral envelope function formalism applied to broken gap tunnel field-effect transistors

D. Verreck*, M. Van de Put†, A.S. Verhulst, B. Sorée †*, W. Magnus†,
A. Dabral*, A. Thean and G. Groeseneken*
imec, Kapeldreef 75, 3001 Leuven, Belgium
*Department of Electrical Engineering, KU Leuven, Belgium
†Department of Physics, Universiteit Antwerpen, Belgium
e-mail: devin.verreck@imec.be

A carefully chosen heterostructure can significantly boost the performance of tunnel field-effect transistors (TFET) [1], [2]. Modelling of these hetero-TFETs requires a quantum mechanical (QM) approach with an accurate band structure to allow for a correct description of band-to-band-tunneling (BTBT). Reflections at the heterojunction, as well as field-induced and size-induced confinement, also need to be considered, as they can heavily influence TFET performance. We have therefore developed a fully QM 2D solver, combining for the first time a full zone 15-band envelope function (EF) formalism with a spectral approach, including a heterostructure basis set transformation.

Our formalism is based on the EF formalism with quantum transmitting boundary conditions [3]. In going to a 15-band description, we replace the finite difference (FD) scheme in the confined direction with a spectral approach, in which we expand the odd (F_n) and even (F_m) EFs, and the external potential V_e as follows:

$$F_n(x,z) = \sum_{\mu=-\infty}^{+\infty} \tilde{F}_n(x,k_{z\mu})\sin(k_{z\mu}z) \quad (1)$$

$$F_m(x,z) = \sum_{\mu=-\infty}^{+\infty} \tilde{F}_m(x,k_{z\mu})\cos(k_{z\mu}z) \quad (2)$$

$$V_e(x,z) = \sum_{\mu=-\infty}^{+\infty} \tilde{V}_e(x,k_{z\mu})\cos(k_{z\mu}z) \quad (3)$$

with x (z) the transport (confinement) direction, and translational invariance in y. The parity of the EFs is determined by the band coupling. Inserting Eqs. (1)-(3) in the EF system finally results in the system in Fig. 1. If N_x x-grid points, N bands and N_{k_z} spectral components are considered, the system has dimensions $N_x \times N_{k_z} \times N$ after discretization, instead of $N_x \times N_z \times N$ in a FD approach. Since spectral methods provide exponential accuracy, compared to only polynomial accuracy for FD, N_{k_z} can be much lower than N_z, especially when the EFs vary slowly in the confined z-direction. Additionally, the cut-off in the spectral expansion prevents highly oscillating out-of-zone spurious solutions from polluting the first Brillouin zone (see Fig. 2). Fig. 3 shows the full simulation procedure.

In order to use the same EF basis set throughout the heterostructure, the matrix elements $\mathbf{p}_{nm}$ and H_{nm} (see Fig. 1) are transformed [3]. This transformation requires a common eigenvalue decomposition, and therefore commutativity, of the momentum matrices. For the exact case of infinite bands, this is satisfied. Momentum matrix elements in literature for finite band models, however, have lost this feature in the fitting process. We have therefore developed a constrained optimization algorithm, to search for **k**·**p**-parameters that reproduce the most relevant band structure features, while retaining commutativity of the momentum matrices, hence allowing for a basis set transform (see Fig. 4).

Figs. 5 and 6 show simulation results for a broken gap diode and p-n-i-n TFET. The wider body device has a deteriorated SS as a result of poorer electrostatic gate control. The EF formalism allows for a transparent analysis of the transmission spectra of individual subband modes (see Fig. 5). The computational efficiency of the spectral method permits the simulation of wide structures: one 30 nm body TFET biaspoint only takes about 15 min using 10 cores on a state-of-the-art server.

In conclusion, we showed a full-zone EF formalism using a spectral method, along with a constrained optimization to obtain **k**·**p**-parameters that retain commutativity of the momentum matrices. We demonstrated the formalism for hetero-diodes and TFETs, highlighting the transparency of the analysis and the computational efficiency compared to existing QM BTBT solvers.

D.Verreck acknowledges support by IWT-Vlaanderen. This work was supported by imec's Industrial Affiliation Program.

[1] H. Lu *et al*., IEEE J. Elec. Dev. Soc. **2**, 44-49 (2014).
[2] U. Avci *et al*., IEEE J. Elec. Dev. Soc. **99**, 1 (2015).
[3] D. Verreck *et al*., J. Appl. Phys. **115**, 053706 (2014).
[4] S. Ben Radhia *et al*., Semicond. Sci. Technol. **22**, 4 (2007).

$$
\begin{aligned}
\frac{-\hbar^2}{2m_e}\frac{\partial^2 \tilde{F}_n(x,k_{z\mu})}{\partial x^2} &+ k_y^2\frac{\hbar^2}{2m_e}\tilde{F}_n(x,k_{z\mu}) + k_{z\mu}^2\frac{\hbar^2}{2m_e}\tilde{F}_n(x,k_{z\mu}) \\
&- \frac{i\hbar}{m_e}\sum_{m''}\{\mathbf{p}_{nm''}(x)\}_x\frac{\partial \tilde{F}_{m''}(x,k_{z\mu})}{\partial x} \\
&+ k_y\frac{\hbar}{m_e}\sum_{m'}\{\mathbf{p}_{nm'}(x)\}_y\tilde{F}_{m'}(x,k_{z\mu}) \\
&\pm k_{z\mu}\frac{i\hbar}{m_e}\sum_{m}\{\mathbf{p}_{nm}(x)\}_z\tilde{F}_{m}(x,k_{z\mu}) \\
&+ \sum_{m'''}H_{nm'''}(x)\tilde{F}_{m'''}(x,k_{z\mu}) \\
+ \sum_{\mu'=0}^{+\infty}&\left[\tilde{V}_e(x,k_{z\mu'}-k_{z\mu}) \mp \tilde{V}_e(x,k_{z\mu'}+k_{z\mu})\right]\tilde{F}_n(x,k_{z\mu}) \\
&= E\tilde{F}_n(x,k_{z\mu}),
\end{aligned}
$$

Fig. 1. System of EF equations after the spectral transform. The plus(minus)-sign in the potential term corresponds to an even(odd) EF. m_e is the free electron mass. $\mathbf{p}_{nm}$ and H_{nm} represent the $\mathbf{k}\cdot\mathbf{p}$ interband momentum and Hamiltonian matrix elements respectively, which couple band n to band m. Note that the potential term becomes the sum of a convolution and an autocorrelation of the spectral components of the potential.

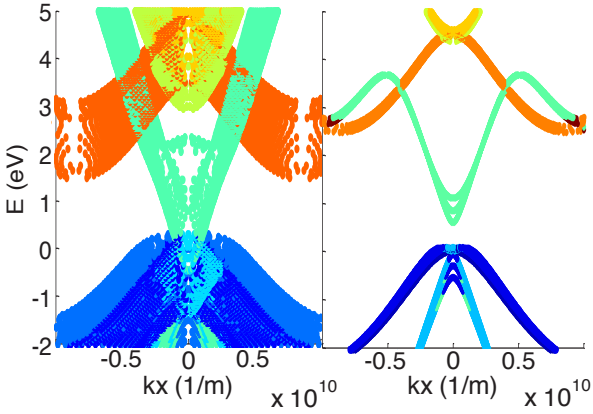

Fig. 2. 15-band confined band structure calculation for a 10 nm InAs slab using a finite difference scheme (left) and a spectral approach with 3 spectral components (right) in the confined z-direction. The spectral approach prevents spurious solutions from folding back onto the zone center and hence results in a correct confined band structure description. Colors indicate the dominant band contribution to each state.

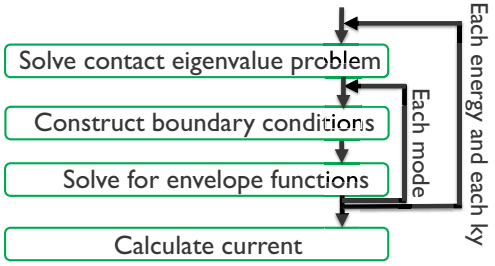

Fig. 3. Flowchart of the developed formalism.

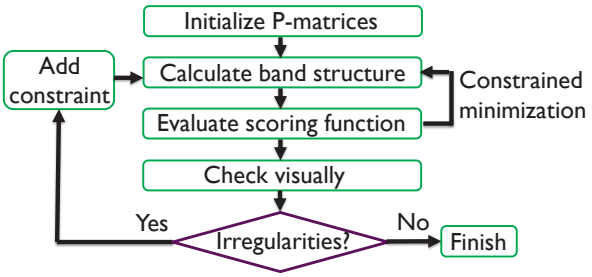

Fig. 4. Parameter search algorithm. The scoring function is a weighted sum of differences of calculated and experimental values from literature of effective masses and bandgaps at the Γ, X-and L-valleys. The constraints ensure commutativity of the momentum matrices P_x, P_y and P_z.

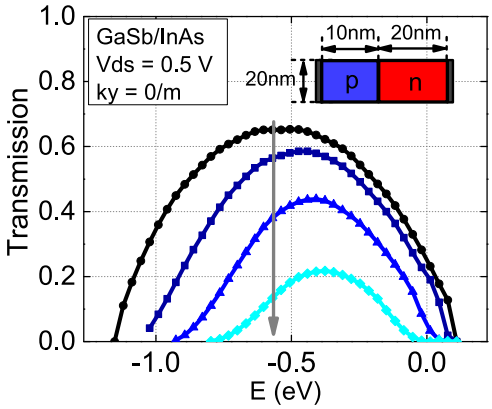

Fig. 5. Individual subband transmission probabilities at $k_y = 0$ for a broken gap diode, illustrating the transparant data analysis. Parameters have been obtained with the algorithm in Fig. 4. Doping is 5x10^{19} cm^{-3} in the p- and n-regions. The arrow indicates increasing subband number.

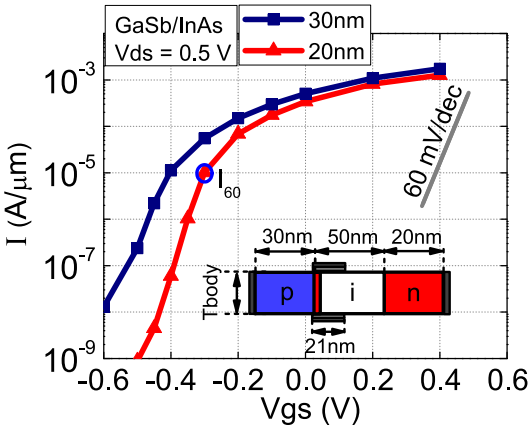

Fig. 6. I-V curves for broken gap p-n-i-n TFETs with Tbody 30 nm and 20 nm. One I-V curve is generated in about 2.5 h on a 10 core server, allowing for an efficient architecture optimization. Source, pocket and drain doping are 1x10^{19} cm^{-3}, 1x10^{19} cm^{-3} and 5x10^{17} cm^{-3} respectively. Pocket thickness is 1 nm. The gate stack has an equivalent oxide thickness of 0.6 nm and a metal workfunction of 4.5 eV.